Bioresource Technology 414 (2024) 131562

Contents lists available at ScienceDirect

Bioresource Technology

journal homepage: www.elsevier.com/locate/biortech

Influence of pyrolysis time on removal of heavy metals using biochar derived from macroalgal biomass (*Oedogonium* sp.)

Anjon Kumar Mondal, Cora Hinkley, Stalin Kondaveeti, Phong H.N. Vo, Peter Ralph, Unnikrishnan Kuzhiumparambil *

Climate Change Cluster, University of Technology Sydney, Ultimo, NSW 2007, Australia

HIGHLIGHTS

- Pyrolysis is applied at different times to convert *Oedogonium* biomass into biochar.
- Pyrolysis time affected on biochar properties and removal of heavy metals.
- Biochar obtained from a 40 min pyrolysis time exhibits higher removal efficiency.
- The Langmuir isotherm and PSO model are fitted to explain the adsorption mechanism.

GRAPHICAL ABSTRACT

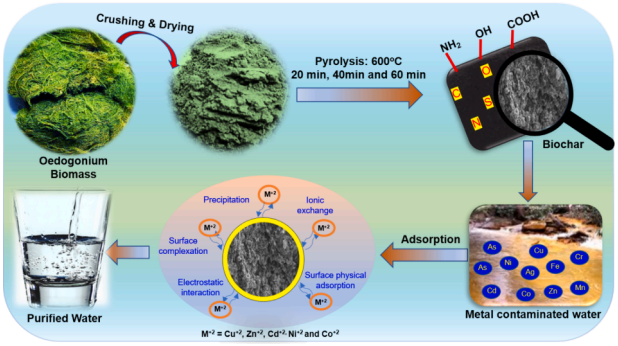

ARTICLE INFO

Keywords:
Pyrolysis
Oedogonium
Biochar
Adsorption efficiency
Heavy metals

ABSTRACT

In this study, pyrolysis was performed at different times to convert *Oedogonium* biomass into biochar. The physicochemical properties show that the pyrolysis time significantly impacts structural and morphological changes in biochar samples. The influence of pyrolysis time on the removal of multiple heavy metals was investigated. Owing to the presence of abundant functional groups, inorganic minerals and porous nature, biochar obtained from a 40 min pyrolysis time showed higher removal efficiency of heavy metals compared to biochars pyrolyzed at 20 mins and 60 mins even with higher concentrations of metal ions. The maximum adsorption capacity was observed 9.33, 10.74, 322.58, 13.70 and 9.11 mg/g with the biochar prepared at the pyrolysis time of 40 mins for Co, Ni, Cu, Zn and Cd, respectively. The adsorption isotherm is well fitted with the Langmuir adsorption model for heavy metals adsorption, and the kinetic study is well-defined by a pseudo second-order model.

1. Introduction

With the rapid population growth, industrial development and urbanization, water shortage and pollution are becoming significant global challenges (Truong et al., 2023; Wang et al., 2023). Our global ecosystems are now under alarming threat because of the simultaneous

* Corresponding author.
E-mail address: Unnikrishnan.kuzhiumparambil@uts.edu.au (U. Kuzhiumparambil).

https://doi.org/10.1016/j.biortech.2024.131562
Received 24 June 2024; Received in revised form 18 September 2024; Accepted 30 September 2024
Available online 30 September 2024

increase of toxic heavy metals and other contaminants in water and land resources (Chowdhury et al., 2016; World Health, 2022). Various industries, including electronics, batteries, metal processing and metallurgy, tanning and fabric dying and petrochemical processing, are generating large quantities of inorganic and organic contaminants and heavy metals that harm human health and ecosystems. Because of their non-decomposable and bio-accumulating characteristics, heavy metals are regarded as the most harmful pollutants, creating severe health effects, including damage to the kidney, liver, and nervous systems in humans (Katiyar et al., 2021). Discharge of heavy metals containing wastewater into water bodies can cause serious health risks for aquatic life (Liao et al., 2018). The levels of different heavy metal concentration detected in the surface water bodies throughout the world ranges from 0.001 mg/L to 3.995 mg/L (Kumar et al., 2019). Thus, removing heavy metals from wastewater resources is an urgent concern to meet safety standards before they are discharged into the environment.

Currently, removing toxic heavy metals from wastewater relies on the following strategies: precipitation, complexation, electrochemical treatment, reverse osmosis, ion exchange, and membrane separation (Carolin et al., 2017). However, high processing costs, ineffective heavy metals removal and complex operation of these conventional methods limit their large-scale applications (Kehrein et al., 2020). Adsorption is the most effective technique for removing heavy metals as it has several advantages over other techniques, including higher removal efficiency, ease of operation, and low operational cost (Staszak & Regel-Rosocka, 2024). The adsorption process can facilitate the diffusion of heavy metal ions into pores of adsorbent substrates and get shifted into the vacant active surfaces until reaching equilibrium (Ahmad et al., 2013). Several adsorbents have been used to remove heavy metals, including graphene, nanotubes, activated carbon, nanocomposites and modified cellulose (Bilal et al., 2021). However, most are expensive to manufacture and not industrially feasible.

Over the past decades, the primary focus has been developing low-cost green adsorbents for removing heavy metals. Biochar has attracted substantial attention to meet the requirement for removing heavy metals from different wastewaters because of its cost-effectiveness and removal efficiency (Xiang et al., 2020). Biochar is a solid carbonaceous material, one of the primary products produced from the pyrolysis of biomasses (Qiu et al., 2021). Recently, biochar is regarded as an effective substitute for activated carbon (Alhashimi & Aktas, 2017). In previous reports, various feedstocks, such as wheat straw, rice husk, macroalgae, microalgae, grass, coffee husk, and waste sludge, have been assessed for the synthesis of biochar (Oliveira et al., 2017). Among them, macroalgae and microalgae are third-generation feedstocks that have recently focused on producing biochar due to their availability and the waste residuals from the rising industry after collecting the main products (Yu et al., 2017).

Algal biochar has intrinsic properties, including porous structure with a combination of macro, meso and micropores, inorganic mineral contents (K, Ca, Na, P and Mg), hydrophilic characteristics and diversity of surface binding oxygen-containing functional groups (–OH, − COOH, C = O) (Cho et al., 2023). These properties promote algal biochar as an effective adsorbent to remove organic and inorganic pollutants from wastewater resources. Pyrolysis, a thermochemical method, converts biomasses into biochar (Lyu et al., 2016). Pyrolysis conditions (pyrolysis time and temperature) and biomass type play a key role in developing the physicochemical properties of biochar for a desired application (Arán et al., 2023; Wang et al., 2019b). Significant research has been directed to synthesize macroalgae-based biochar using different pyrolysis temperatures and apply these biochars to remove heavy metals and other contaminants. However, most of the reports ignore the influence of pyrolysis time of macroalgae-based biochar on the adsorption efficiency of heavy metals. Algae-based biochar does not show the expected physical and chemical properties including surface area, surface structure and functional groups at the temperature less than 600 ℃. When the temperature increased to more than 600 ℃, the biochar does not contain porous and disordered structure as expected, which results in the decrease of surface area (Tan et al., 2023).

In the current study, *Oedogonium* biomass has been used to prepare biochar and investigated for its removal capacity of five toxic heavy metals (Co, Ni, Cu, Zn and Cd) from aqueous solution. This study aims to develop biochars from *Oedogonium* species at the fixed temperature of 600 ℃ with different pyrolysis times (20, 40 and 60 mins) and characterize their physical and chemical properties, including chemical composition, surface morphology, and functional groups before applying biochars for the removal of heavy metals. In addition, the influence of pyrolysis time on adsorption and the effect of other operational parameters, including the concentration of heavy metals, contact time, adsorption isotherm and kinetics, were studied to define the adsorption mechanism of five heavy metals on *Oedogonium*-derived biochar.

2. Experimental

2.1. Chemicals and macroalgae

Analytical grade reagents and chemicals were used in this study. Standard solutions of Co, Cu, Ni, Cd and Zn were used to prepare all standard curves. Multiple heavy metals stock solutions were prepared by dissolving cobalt chloride (II) hexahydrate ($CoCl_2{\cdot}6H_2O$), nickel (II) sulphate hexahydrate ($NiSO_4{\cdot}6H_2O$), copper (II) sulphate pentahydrate ($CuSO_4{\cdot}5H_2O$), cadmium chloride ($CdCl_2$) and zinc sulphate heptahydrate ($ZnSO_4{\cdot}7H_2O$) in the concentration of 25, 50, 100, 200 and 500 mg/L of each metal salt in MQ water. The pH of the metal salt solutions was adjusted to 5.0 with hydrochloric acid.

Oedogonium sp. was collected from a commercial seaweed farm in Queensland, Australia. It was washed three times using de-ionised (DI) water and dried in an oven at 60 ℃ for 24 h. The dried *Oedogonium* was ground into powder using a grinder and sieved with 0.25 mm sieve.

2.2. Biochar preparation

Oedogonium-derived biochar was prepared by using our previous report (Mondal et al., 2024). The only change was the use of different pyrolysis times. In brief, 50 g of powder was placed in porcelain crucibles (N = 3) and pyrolysed in a horizontal tube furnace (Lab Tech, Model STF1200) at 600 ℃ with different pyrolysis times (20, 40 and 60 mins) with N_2 flow (3.5 L/min) and the ramp rate of 20 ℃/min. N_2 was passed for at least 20 mins before starting heating and continued throughout and after the pyrolysis until the furnace's inside temperature reached less than 100 ℃. The material was cooled to room temperature and collected in plastic jars for analysis. For convenience, *Oedogonium*-derived biochar was designated Oed-20, Oed-40, and Oed-60, depending on their pyrolysis time.

2.3. Characterization

Oedogonium biomass and biochar samples were characterised by using different analytical techniques. The elemental composition in *Oedogonium*-derived biochar samples and heavy metals content before and after adsorption were analysed using MP-AES (Agilent Technologies 4210 MP-AES) and ICP-MS (Agilent Technologies 7700 ICP-MS), respectively. CN analyser (LECO 630–300-400) was employed to analyze the percentages of C and N and C:N ratio. To measure the pH by a pH meter (inoLab pH level 2, Germany), 2 g of biochar was dispersed in 20 mL of MQ water (1 W:10 V) and shaken for 20 mins. A scanning electron microscope (SEM) (Zeiss EVO LS15) coupled with energy-dispersive X-ray spectroscopy (EDS) was employed to observe the surface morphology of *Oedogonium* biomass and biochar pyrolyzed at different pyrolysis times. The specific surface area and porosity were examined using Brunauer-Emmett-Teller (BET) nitrogen adsorption–desorption isotherms and the Barrett-Joyner-Halenda (BJH)

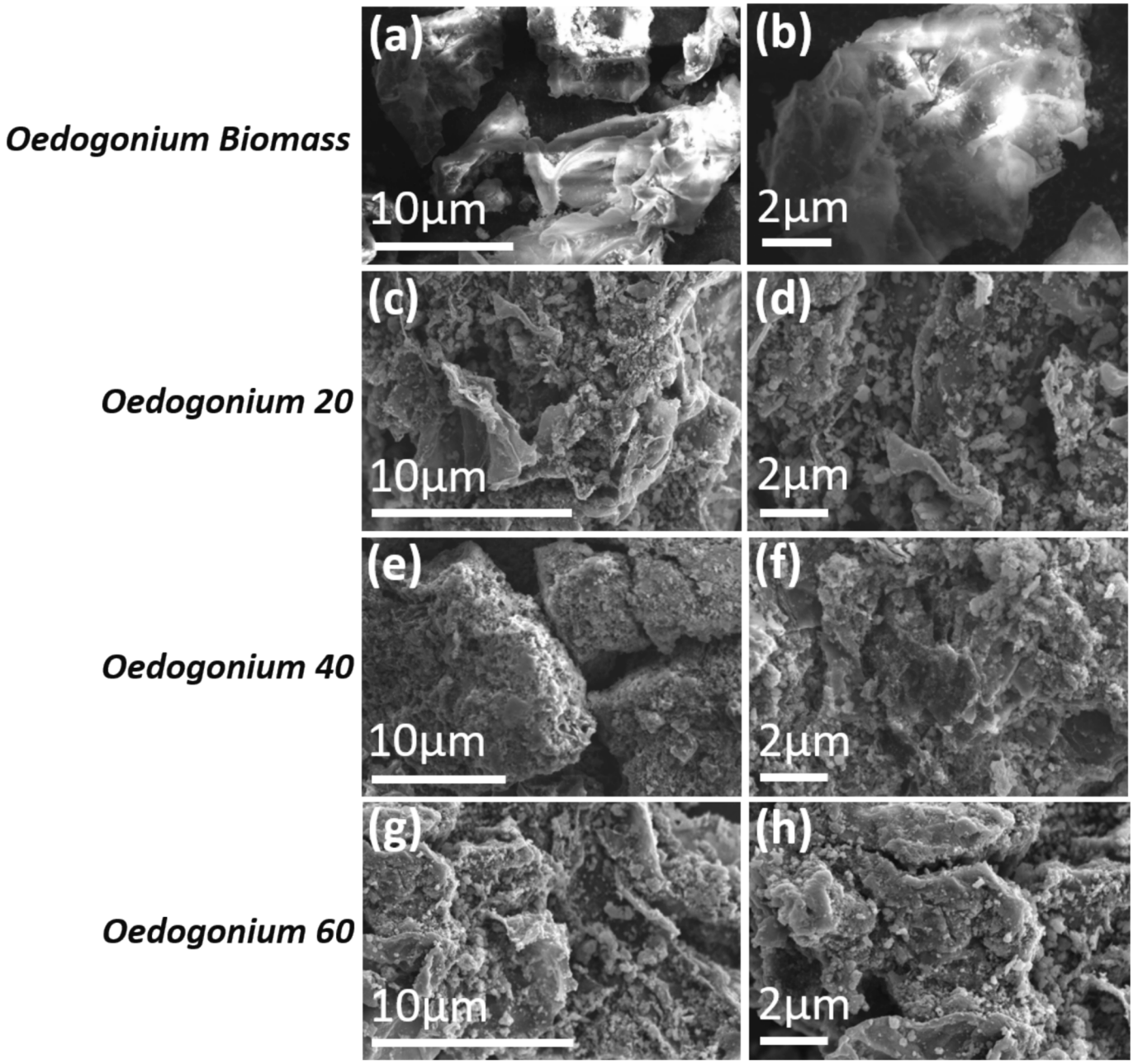

Fig. 1. SEM images of *Oedogonium*-derived biomass and biochars: *Oedogonium* biomass: (a) low magnification (b) high magnification; *Oedogonium* 20: (c) low magnification (d) high magnification; *Oedogonium* 40: (e) low magnification (f) high magnification *Oedogonium* 60 (g) low magnification (h) high magnification.

method, respectively by using a Micromeritics 3 Flex™ surface characterization analyzer at 77 K. The surface functional groups were examined using a Fourier transform infrared spectrometer (FTIR) at ATR mode (Nicolet FT-IR 6700). The spectra were recorded between the range of 4000 to 400 cm^{-1} wavelength. The crystalline structure was determined using X-ray diffraction (XRD) (Bruker D8 DISCOVER), and the samples were scanned in the range of 2θ from 10 to 80° with a scan speed of 5°/min. Thermogravimetric analysis (TGA) (TA Instrument SDT Q600-1255) was carried out to determine the thermal stability of samples. Raman Spectroscopy (ThermoScientific DXR3 SmartRaman) was used to determine the structural evaluation of biochar samples at an excitation wavelength of 532 nm.

2.4. Adsorption experiments of heavy metals

Batch experiments were conducted to evaluate the adsorption capacity and removal efficiency for all biochar samples (Oed-20, Oed-40 and Oed-60). 100 mL of heavy metals stock solution from the concentration of 25 mg/L was taken in three different 250 mL conical flask (100 mL in each conical flask). 500 mg of each biochar sample (Oed-20, Oed-40 and Oed-60) were added to three conical flasks and positioned on electric shaker at 150 rpm for 24 h. After 24 h, all three solutions were collected by centrifuge, and the solutions were further filtered by 0.20 µm syringe filter. To evaluate the maximum adsorption efficiencies of Oed-20, Oed-40, and Oed-60, 500 mg/L stock solution was used, and 500 mg of each biochar was used, followed by the similar process as mentioned above. The heavy metals stock solution and filtered solutions were diluted by 1 % HNO_3 and analysed by using ICP-MS (Agilent Technologies 7700 ICP-MS).

The adsorption capacity and removal efficiency of multiple heavy metals in biochar samples were calculated by the following equations: (Jaiswal et al., 2021b)

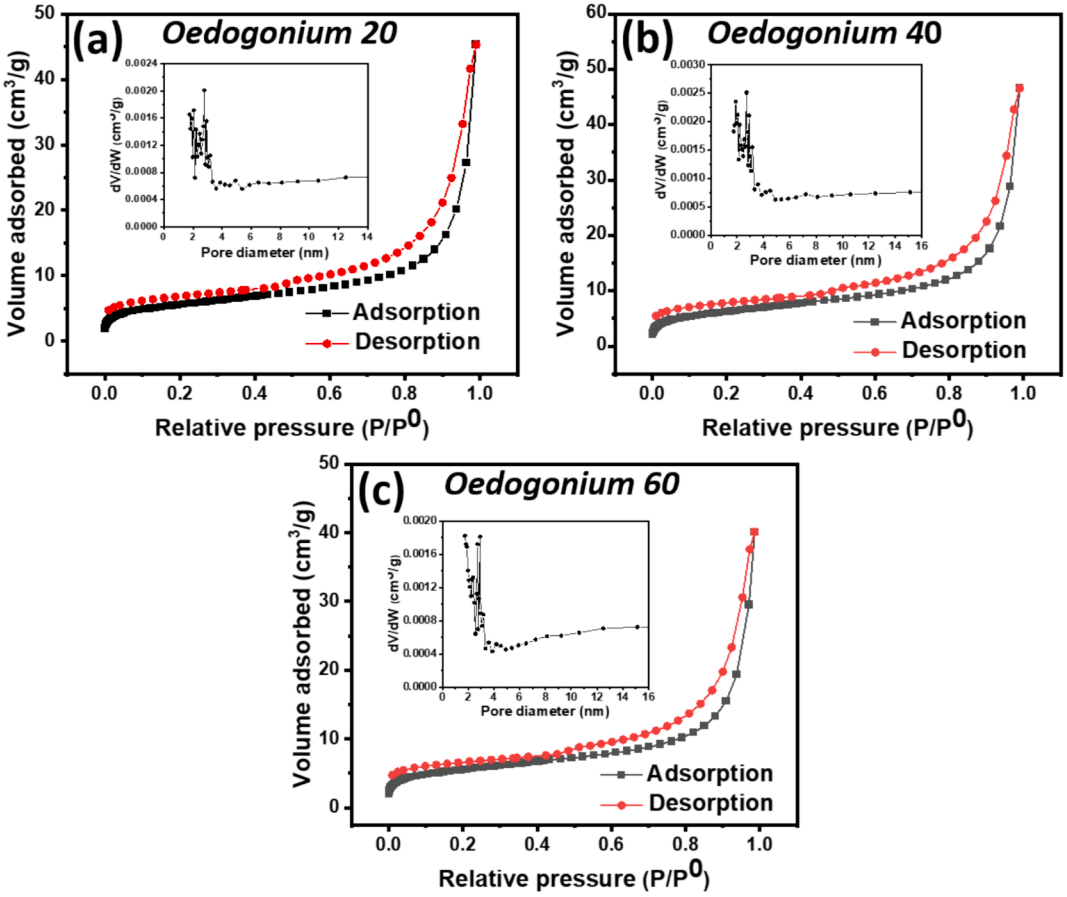

Fig. 2. Nitrogen adsorption/desorption isotherms and corresponding BJH pore size distributions (inset) of (a) *Oedogonium 20* (b) *Oedogonium 40* and (c) *Oedogonium 60*.

Table 1
Elemental composition of *Oedogonium*-derived biochars.

Parameters	Units	*Oedogonium 20*	*Oedogonium 40*	*Oedogonium 60*
Carbon (C)	%	68.39	70.23	69.80
Nitrogen (N)	%	7.80	7.91	7.89
C/N ratio	na	8.77	8.88	8.85
Oxygen (O)	%	20.41	21.75	20.41
O/C ratio	na	0.30	0.31	0.29
(O + N)/C	na	0.41	0.42	0.41
Ca	g/kg	75.14	127.94	9.92
Na	g/kg	32.18	48.95	29.21
K	g/kg	68.61	90.78	10.92
Mg	g/kg	30.06	5.57	5.65
P	g/kg	41.5	48.63	50.45

na = not applicable.

$$\text{Adsorption capacity } (q_e) = (C_0 - C_e) \times V/m \quad (1)$$

$$\text{Removal efficiency } (\%) = (C_0 - C_e)/C_0 \times 100 \quad (2)$$

where, C_0 is the primary concentration and C_e is the final/equilibrium concentration of non-adsorbed heavy metals, while V (mL) is the volumes of solutions and m (mg) is the mass of the biochar.

2.5. Adsorption isotherm

The linear form of Langmuir and Freundlich isotherm can be expressed according to Eq. (3) and Eq. (4): (Jaiswal et al., 2021a)

$$C_e/q_e = 1/K_L q_m + C_e/q_m \quad (3)$$

$$\ln q_e = \ln K_F + 1/n(\ln C_e) \quad (4)$$

where, C_e and q_e is the concentration and adsorption capacity, respectively at equilibrium, K_L is the Langmuir adsorption constant (L/mg), q_m is the maximum adsorption capacity and K_F and n are the Freundlich constants related to the adsorption capacity and adsorption intensity, respectively. K_L, K_F, q_m, and n can be calculated from the slope and intercept from the linear fitting C_e/q_e versus C_e.

2.6. Adsorption kinetics

The mathematical formula of the Pseudo-first-order (PFO) and Pseudo-second-order (PSO) kinetic models are presented in equation (5) and (6), respectively (Verma et al., 2020).

$$\ln(q_e - q_t) = \ln q_e - k_1 t \quad (5)$$

$$t/q_t = 1/k_2 q_{e2} + t/q_e \quad (6)$$

where, q_e is the adsorbed amounts (mg/g) of metal ions at equilibrium and q_t is the adsorbed amounts (mg/g) at time t. k_1 and k_2 are the rate constant of the adsorption of PFO and PSO, respectively.

3. Results and discussion

3.1. Biochar properties

3.1.1. Surface morphology of Oedogoium biomass and biochar

Scanning electron microscopy (SEM) was used to observe the structural morphology of *Oedogonium* biomass and biochars. Fig. 1 illustrates

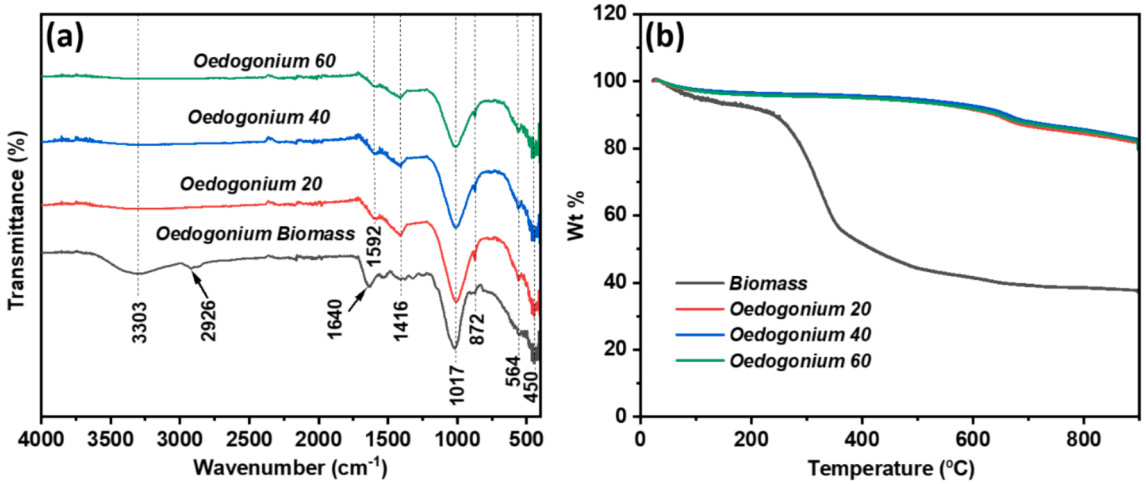

Fig. 3. (a) FTIR spectra and (b) TGA curves of *Oedogonium*-derived biomass and biochars.

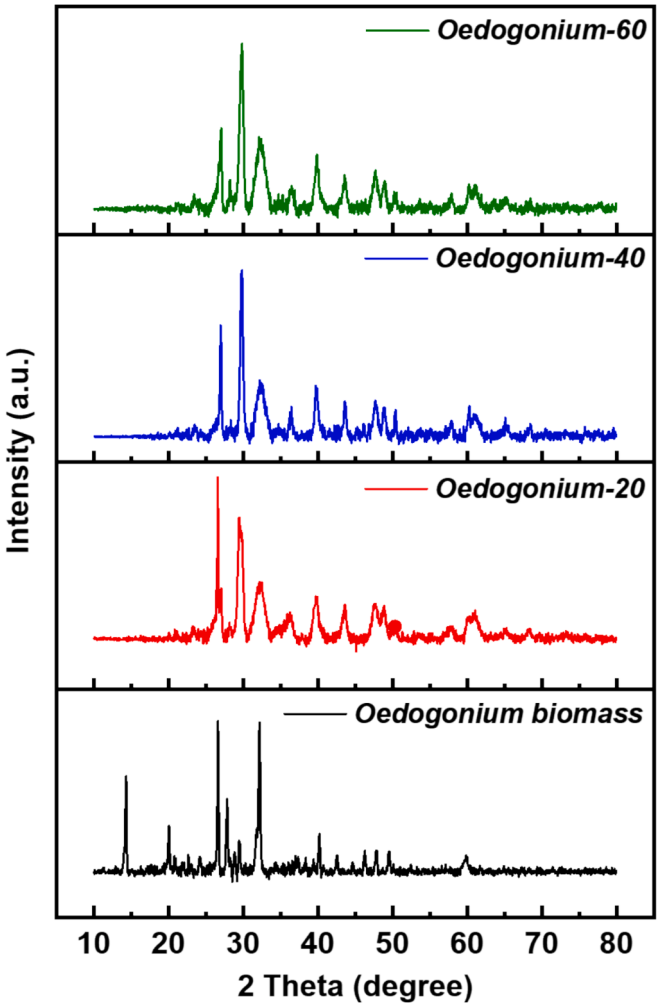

Fig. 4. X-ray diffraction patterns of biomass and biochar samples obtained from *Oedogonium* sp.

the low and high-magnification SEM images of biomass and prepared biochars. The surface morphology of *Oedogonium* biomass presents intact regular shapes and unbroken surfaces (Fig. 1(a) and 1(b)). The surface structure of biochars prepared from *Oedogonium* biomass at different pyrolysis times revealed irregular and damaged shapes with distorted surfaces because of the volatilization of organic components (Fig. 1(c)-1(h)) (Jaiswal et al., 2021a). Due to the condensation of organic hydrocarbons such as tars and the consecutive disintegration of pyrolyzed products at 600 ºC, all biochar samples generated irregular and distorted structures. However, as shown in Fig. 1(e) and 1(f), Oed-40 displays more porous and disordered structure compared to Oed-20 (Fig. 1(c) and 1(d)) and Oed-60 (Fig. 1(g) and 1(h)). It can be elucidated that more organic substances were thermally decomposed, and more volatile matter was released from engraving pores during the pyrolysis time of 40 mins (Oed-40) than 20 mins (Oed-20). This process increases channels, cavities, pores and distorted structures in the Oed-40 biochar, which is believed to be advantageous for removing heavy metals (Biswal & Balasubramanian, 2023).

The specific surface area and porosity is the vital physical factor of biochar, which affects heavy metal adsorption. Fig. 2 shows the nitrogen adsorption–desorption isotherm of biochars at the pyrolysis time of 20 40 and 60 mins. All biochar samples show type IV isotherms with an apparent hysteresis loop, which indicate a mesoporous nature of the materials (Shaikh et al., 2022). The BET surface area of Oed-20, Oed-40 and Oed-60 are calculated to be 20.21, 22.63 and 19.82 m^2/g, respectively. The total pore volume found to be 0.003, 0.072 and 0.003 cm^3/g. As presented in the insets of panels (a), (b) and (c) in Fig. 2, mesoporous structures of all biochar samples further confirmed by BJH pore size distribution results. The pore size distributions show a narrow distribution with most of the pores in the range of 1.75 to 6 nm, indicating the presence of micro- and mesopores. According to the previous report, the surface area and porosity increased when the pyrolysis time increased. However, increased pyrolysis time causes defects and pores to collapse, which results in the decrease of biochar's surface area (Wang et al., 2019b). In the current study, Oed-40 shows the highest SSA and pore volume compared to Oed-20 and Oed-60. Due to the higher SSA, pore volume and micro-mesoporous structure, Oed-40 could have more adsorption efficiency than that of Oed-20 and Oed-60.

3.1.2. Elemental analysis

The elemental analysis results (Table 1) demonstrated that the *Oedogonium* biochars consist of carbon (68.4–70.2 %), oxygen (20.4–21.7 %) and nitrogen (7.80–7.91). The O/C and (O + N)/C ratio are the indication of degree of polarity and aromaticity of biochar. (Chaudhary et al., 2023). The biochar's high O/C and (O + N)/C ratio indicate increased hydrophilicity and polar functional groups. The polar functional groups actively participate in the adsorption of heavy metals (Truong et al., 2023). In the current study, the O/C and (O + N)/C ratio of Oed-40 biochar were higher than Oed-20 and Oed-60 (Table 1). The C/N ratio is also a vital parameter in adsorption of heavy metals.

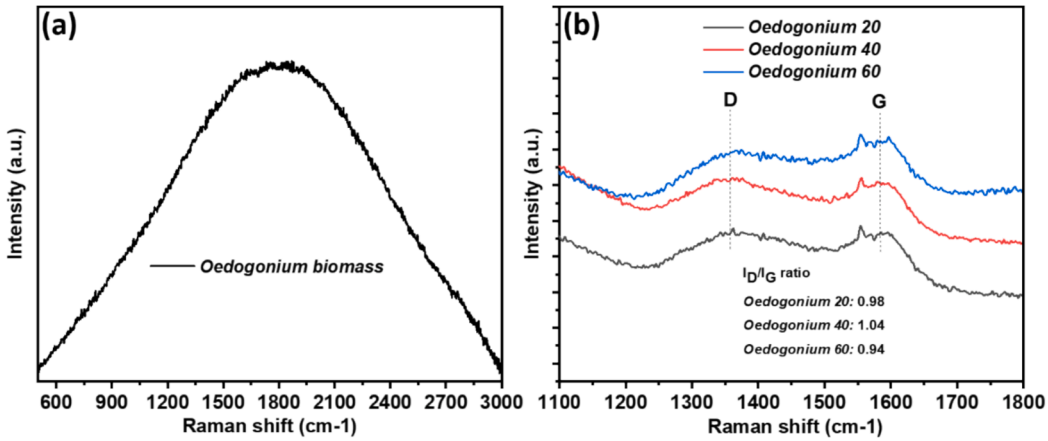

Fig. 5. Raman spectra of *Oedogonium*-derived (a) biomass and (b) biochars at different pyrolysis time.

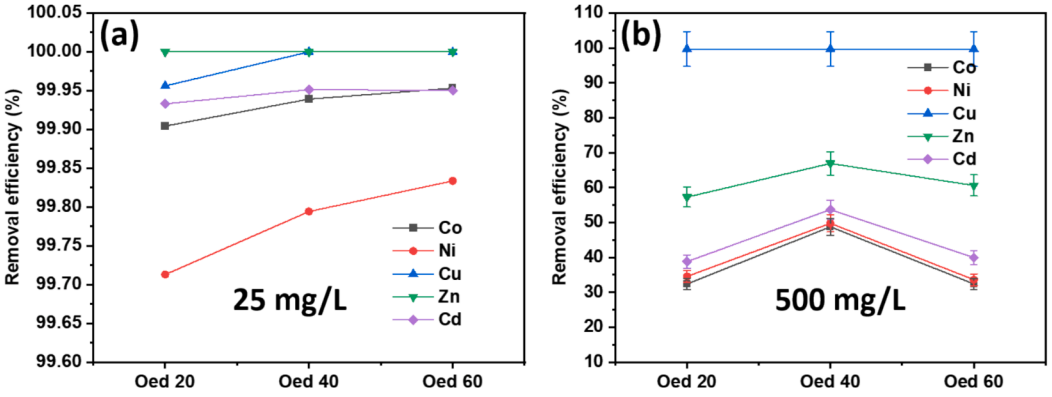

Fig. 6. Removal efficiency of heavy metals from the multiple heavy metal salt solution by Oed-20, Oed-40 and Oed-60 biochars: (a) Initial metal ions concentration 25 mg/L, initial pH = 5 and biochar dose = 500 mg; (b) Initial metal ions concentration 500 mg/L, initial pH = 5 and biochar dose = 500 mg.

Generally, the biochar with a high C/N ratio is rich in carbohydrates, where the dominant functional groups are mainly carboxylic (Sanka et al., 2020). In this study, Oed-40 showed a higher C/N ratio of 8.88 compared to Oed-20 (8.77) and Oed-60 (8.85). These indicate that the Oed-40 will have a better adsorption capacity of heavy metal ions than Oed-20 and Oed-60. The higher C/N ratio achieved at high temperatures and prolonged pyrolysis time is due to the release of N-containing functional groups (Sanka et al., 2020). Available inorganic minerals such as K, Ca, Na, P and Mg in all biochar samples could enhance the adsorption of heavy metals through the cation exchange phenomenon, where ions from the multiple heavy metal solution exchange similarly charged ions available on biochar (Poo et al., 2018). The ratio of atoms for each element (C, N and O) and atomic ratio of elements are also provided in a separate Table S1 (Suppl inf.).

3.1.3. *Surface functional groups and thermal stability*

FTIR analysis was conducted to identify the functional groups of *Oedogonium* biomass and biochar samples at different pyrolysis times and the characteristic spectra are presented in Fig. 3 (a). The broad peaks located at 3303 cm^{-1} and 2926 cm^{-1} in *Oedogonium* biomass sample, which ascribed to –OH group and methyl C-H stretching, respectively. After pyrolysis at 600 ℃ and different pyrolysis times, the peak intensity of –OH group reduced, which related to the decomposition of alcoholic and phenolic functionalities and the disappearance of aliphatic methyl group indicated that the methyl group was eradicated from the aromatic rings in biochar samples (Jaiswal et al., 2021a). A series of peaks were observed at 1592, 1416 and 1017 cm-1 in biochar samples assigned to the C = O stretching, which endorses the presence of carboxyl groups. This agrees well with the elemental analysis above (Table 1), where a high O/C C/N ratio in Oed-40 biochar indicated a high proportion of carboxyl functional groups. The presence of carboxyl functional groups on the surface of biochar enhances the adsorption capacity of heavy metals (Zhao et al.). The vibration band at 872 cm-1 was assigned to the deformation of aromatic C-H bending and the bands at 564 and 450 cm-1 belonged to C-C stretching, respectively (Singh et al., 2021).

Fig. 3(b) illustrates the TGA curves of *Oedogonium* biomass and biochar samples at different pyrolysis times. The combustion of *Oedogonium* biomass occurred in three different temperature ranges. In the first range (room temperature to 200 ℃), a weight loss of 11 % was found, ascribed to the evaporation of external water attached to the biomass surface and a small quantity of volatile compounds (Roslee & Munajat, 2018). Most of the weight losses (33 %) happened in the second range (200–500 ℃), which is associated with the combustion of proteins, carbohydrates and lipids (Teh et al., 2017). Finally, in the third region (500–900 ℃), a weight loss between 37 and 44 % corresponds to the combustion of solid carbon-rich material to form biochar (Koçer & Özçimen, 2021). Unlike the TGA curve of *Oedogonium* biomass, the weight loss of biochars (Oed-20, Oed-40 and Oed-60) occurred in two steps. The differences between the TGA curves of *Oedogonium* biomass and biochars are due to the degradation of lipids, carbohydrate and protein during the pyrolysis of biomass. As shown in Fig. 3(b), biochar samples showed a moderate weight loss until the temperature reached 600 ℃ in the first step, demonstrating the elimination of adsorbed moisture from the surface of biochar. In the second step, the weight loss between the temperature 600 ℃ to 900 ℃ is due to the combustion of carbonaceous solids (Koçer & Özçimen, 2021). From the TGA curves of biochars, it was found that the total weight loss of Oed-40 (17.23 %) was

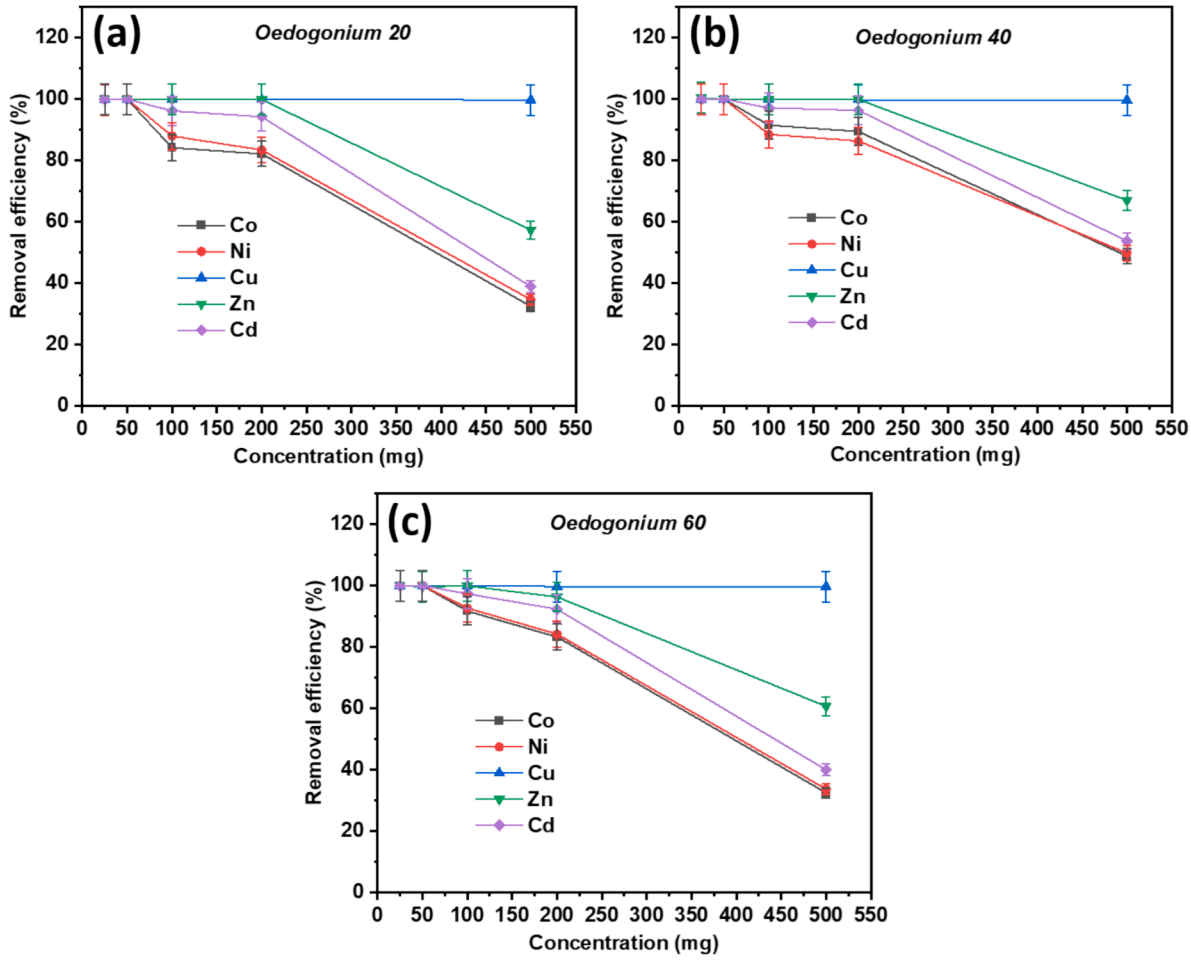

Fig. 7. Effect of initial metal ions concentration on adsorption onto *Oedogonium*-based biochar samples at different pyrolysis times (a) Oed-20 (b) Oed-40, and (c) Oed-60 (initial pH = 5, biochar dose: 500 mg).

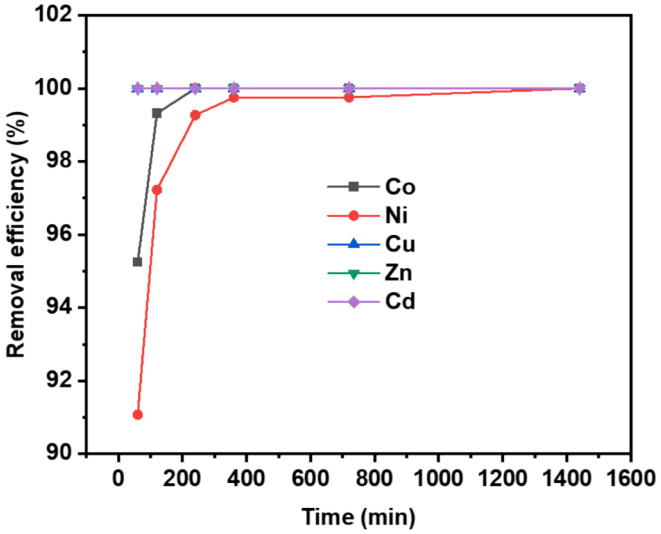

Fig. 8. Removal efficiency of Co (II) Ni (II), Cu (II), Zn (II) and Cd (II) metal ions from the multiple heavy metal solutions by *Oedogonium* biochar (Oed-40) at different time intervals. Initial pH = 5, Biochar dose: 500 mg, and initial metal ions concentration of 25 mg/L (each metal salt).

less than Oed-20 (17.77 %) and Oed-60 (18.53 %), demonstrating that the Oed-40 is thermally more stable than Oed-20 and Oed-60.

3.1.4. X-ray diffraction

XRD patterns of *Oedogonium* biomass and produced biochars at different pyrolysis time of 20, 40 and 60 mins, which are shown in Fig. 4. After pyrolysis at 600 ºC, all biochar samples present numerous sharp and narrow peaks of certain mineral phases (Ca, Na, Mg, P and K) compared to biomass sample. The peaks that appeared at around 29.5°, 36.4°, and 39.7° in biochar samples are ascribed to calcite ($CaCO_3$) contents. The other diffraction peaks observed at 2θ between 30º and 70º are related to minerals such as $CaCO_3$, $MgCO_3$, $Ca_3(PO4)_2$, KCl and NaCl (Jaiswal et al., 2021b). The peaks positioned at 26.9º and 43.5º in biochar samples assigned to the (002) crystal plane of carbon, representing the presence of graphitic structures (Fazal et al., 2021). Minerals on the biochar surface are suitable for exchanging heavy metal ions (Zhao et al., 2019). The EDS spectra and elemental analysis also revealed the presence of different elements with peaks in Oed-20, Oed-40 and Oed-60 (Suppl. Inf. Fig. S1).

3.1.5. Raman analysis

Raman spectroscopy was used to further determine the structure of *Oedogonium* biomass and biochar. Raman spectra of biochar samples encompass two prominent bands: D band (1320–1380 cm^{-1}) and G band (1560–1610 cm^{-1}). The D band corresponds to the disordered graphitic structure, while the G band is associated with the graphitic crystalline structure (Jaiswal et al., 2021b). As shown in Fig. 5(a), biomass has no

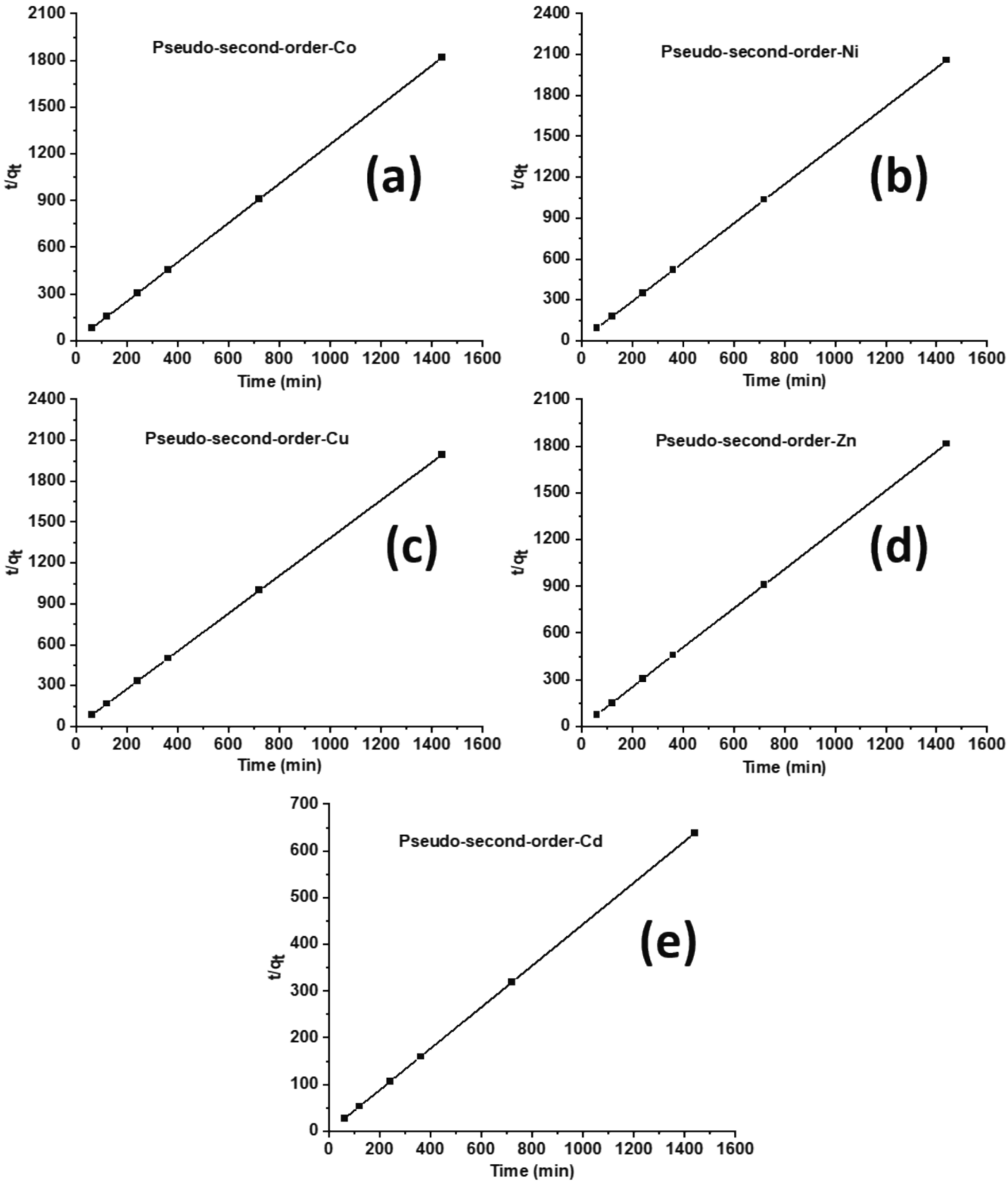

Fig. 9. Pseudo-second-order kinetic models for *Oedogonium*-based biochar (Oed-40).

detectable D and G band; however, biochars (Oed-20, Oed-40 and Oed-60) have a broad D band located at 1356 cm^{-1} and G band at around 1582 cm^{-1} (Fig. 5b).

The I_D/I_G band intensity ratio provides important information about the graphitic degree of carbon. The higher value of I_D/I_G ratio indicates a defective and disordered structure (McDonald-Wharry et al., 2013). In this study, Oed-40 exhibited a higher I_D/I_G ratio (1.04) compared to Oed-20 (0.98) and Oed-60 (0.94), indicating Oed-40 has more defective and disordered structure, which agrees well with the SEM images of Oed-40 (Fig. 1e and f). This type of structure is favourable for increased adsorption properties.

Table 2
Pseudo-first-order and Pseudo-second-order kinetics parameters for multiple heavy metal ions onto Oed-40 biochar.

Biochar	Heavy metals	Pseudo-first-order			Pseudo-second-order		
		q_e (mg g^{-1})	K_1 (min^{-1})	R^2	q_e (mg g^{-1})	K_2 (g mg^{-1} min^{-1})	R^2
Oed-40	Co	0.011	0. 025	0.931	0.793	0.593	1
	Ni	0.045	0. 029	0.929	0.701	0.343	1
	Cu	0.012	0. 026	0.910	0.722	5.989	1
	Zn	0.014	0. 024	0.931	0.793	0.997	1
	Cd	0.19	0. 023	0.912	2.255	3.233	1

3.2. Adsorption of heavy metals

3.2.1. Effect of pyrolysis time on removal efficiency of heavy metals

To investigate the effect of pyrolysis time on the removal of heavy metals, first, we selected low (25 mg/L) and high (500 mg/L) concentration heavy metal solutions to observe the removal efficiency using biochars produced at different pyrolysis times. Fig. 6 illustrates the adsorption results for the removal efficiency of biochars. As shown in Fig. 6(a), at the low concentration (25 mg/L), Oed-20, Oed-40 and Oed-60 showed an excellent removal efficiency of all five heavy metals, between 99.7 % and 100 %. At the low concentration of heavy metals, biochar samples show a higher removal efficiency, which can be ascribed to their surface textural properties and available active sites, which allowed the efficient adsorption of all heavy metals. When the heavy metals concentration was increased to 500 mg/L, the biochar samples showed a different removal efficiency (Fig. 6b). At higher concentration (500 mg/L), the removal efficiency of Cu was as high as 99.7 % for all biochar (Fig. 6b). However, Oed-40 demonstrates a higher removal efficiency of other heavy metals than Oed-20 and Oed-60. These could be attributed to the more active sites available in Oed-40 to adsorb heavy metals than Oed-20 and Oed-60 at higher concentrations (Chaudhary et al., 2023).

3.2.2. Effect of primary concentrations on removal efficiency

The effect of primary concentrations on heavy metal removal provides substantial insight into the race of the five heavy metals throughout the adsorption procedure (Zhao et al.). The investigation was carried out at room temperature by taking a wide range of concentrations of heavy metals (0.1 to 500 mg/L). The pH of the heavy metals solution significantly impacts the adsorption process, which is affected by the surface functional group and surface charge of biochar and the degree of ionization is also affected by the pH (Hoslett et al., 2019). The adsorption capacity and removal efficiency are generally decreased when the pH is low (pH = 2). This is because of the protonation of surface functional groups of biochar at strongly acidic conditions, which produces electrostatic repulsion of positively charged surface functional groups and heavy metal ions. The lower pH also activates the competition between the hydrogen ions and heavy metal ions for active adsorption sites, resulting in low adsorption capacity and removal efficiency (Xiao et al., 2017). When the solution pH increases, the biochar becomes negatively charged and the competition between hydrogen ions and heavy metal ions decreases, which causes increased adsorption capacity and removal efficiency (Jaiswal et al., 2021a). At a pH above 5, heavy metal-like cadmium formed a white precipitation of cadmium hydroxide, interrupting the initial concentration of metal ions and thereby affecting biochars' adsorption capacity and removal efficiency (Park et al., 2017). Based on the reports mentioned above, we adjusted the initial metal solution to pH 5 for adsorption experiments.

The removal efficiency of biochars for five heavy metals are displayed in Fig. S2 and Fig. 7. As shown in Fig. S2, the removal of five heavy metals was 99.48 % to 100 % at low concentrations (0.1–20 mg/L). The heavy metals removal efficiency was 99.6 % to 100 % at the concentration of 25 mg/L and 50 mg/L (Fig. 7). The results demonstrate that plenty of blank active sites available in all biochar samples. The removal efficiency was not significantly decreased at the concentration of 100 mg/L (84.13 % to 99.99 %) and 200 mg/L (88.12 % to 99.86 %), indicating active sites are still available in biochars. The removal efficiency was decreased when the concentration of heavy metal ions in the solution increased to 500 mg/L, which specifies the shortage of effective adsorption sites in the biochar samples. The results also show that all three biochar samples have similar trend for the adsorption of Cu (II) and Zn (II) from all concentrations of heavy metal ions. Nevertheless, the adsorption of Co (II), Ni(II) and Cd(II) metal ions was higher at lower concentrations, while the adsorption was lower at higher concentrations, which is possibly due to the competition among the heavy metals (Jaiswal et al., 2021a). As presented in Fig. 7(a), 7(b) and 7(c), it is clear that the removal efficiency of Oed-40 biochar was higher than Oed-20 and Oed-60, indicating the more available active sites are present in Oed-40 compared to Oed-20 and Oed-60.

In the comparative study of adsorption data in the above experiments, it is evident that the Oed-40 biochar showed the highest removal efficiency compared to Oed-20 and Oed-60 samples. Based on its distinct properties and best performance, the Oed-40 biochar was selected for further experiments, including adsorption isotherms and kinetics. These specific outcomes are discussed in the next sections.

3.2.3. Effect of contact time and adsorption kinetics

To find out the equilibrium, the impact of contact time between the biochar and heavy metals in solutions was studied. To do that, primary concentrations of Co(II), Ni(II), Cu(II), Zn(II) and Cd(II) metal salts solution (25 mg/L each) was used. Experiments were conducted by dispersing 500 mg of biochar in 100 mL of heavy metal salt solution and allowing contact at different time intervals (60, 120, 240, 360, 720 and 1440 min). The kinetic curves of all heavy metals are presented in Fig. 8. It is observed that the adsorption of Cu, Zn and Cd was very fast and adsorbed 100 % in 60 min by Oed-40. The initial adsorption rate of Co (II) and Ni(II) is a bit slower; however, when time increases the adsorption rate increased and reached 100 % at the time of 240 and 1440 mins, respectively. The rapid adsorption of all the heavy metals in the initial stage might be due to the plenty of active sites exist on Oed-40 for the adsorption of heavy metals (Yang et al., 2019).

Adsorption kinetics usually predicts the mechanism of interactions, rate controlling steps and rate of the process. Kinetic analysis was carried out to understand the adsorption behaviours in heavy metal solutions and find an appropriate kinetic model. Two popular kinetic models, pseudo-first-order (PFO) and pseudo-second-order (PSO), are widely used in kinetic studies. The kinetics adsorption tendency of heavy metals can be divided into fast increasing phase and a slow phase to reach the equilibrium. In the first step, the fast phase adsorption occurred on the outer surface of biochar with physical adsorption, while the slow phase adsorption occurred into the micro and mesopores and inner surface of biochar (Liu et al., 2021). The physical procedure controls the PFO model, while PSO is controlled by chemical procedures.

The kinetic plots of PFO and PSO for five heavy metals are displayed in Fig. S3 and Fig. 9, respectively. The results of kinetic parameters are presented in Table 2. It is found that the correlation coefficient (R^2) of PSO is well fitted compared to the correlation coefficient of PFO, indicating the adsorption of heavy metals is a chemical process on Oed-40 biochar by valence forces exchanging or sharing electrons between the biochar and heavy metals (Jaiswal et al., 2021b).

3.2.4. Adsorption isotherm

The adsorption isotherm is mainly used to illustrate the interactions between the adsorbent (*Oedogonium* biochar) and adsorbate (heavy metals) and to understand the adsorption mechanism (Chakraborty et al., 2022). Langmuir and Freundlich isotherm models are mostly used to elucidate the adsorption behaviour of heavy metal ions on biochar.

The linear plot of Langmuir and Freundlich equation of Co, Ni, Cu, Zn

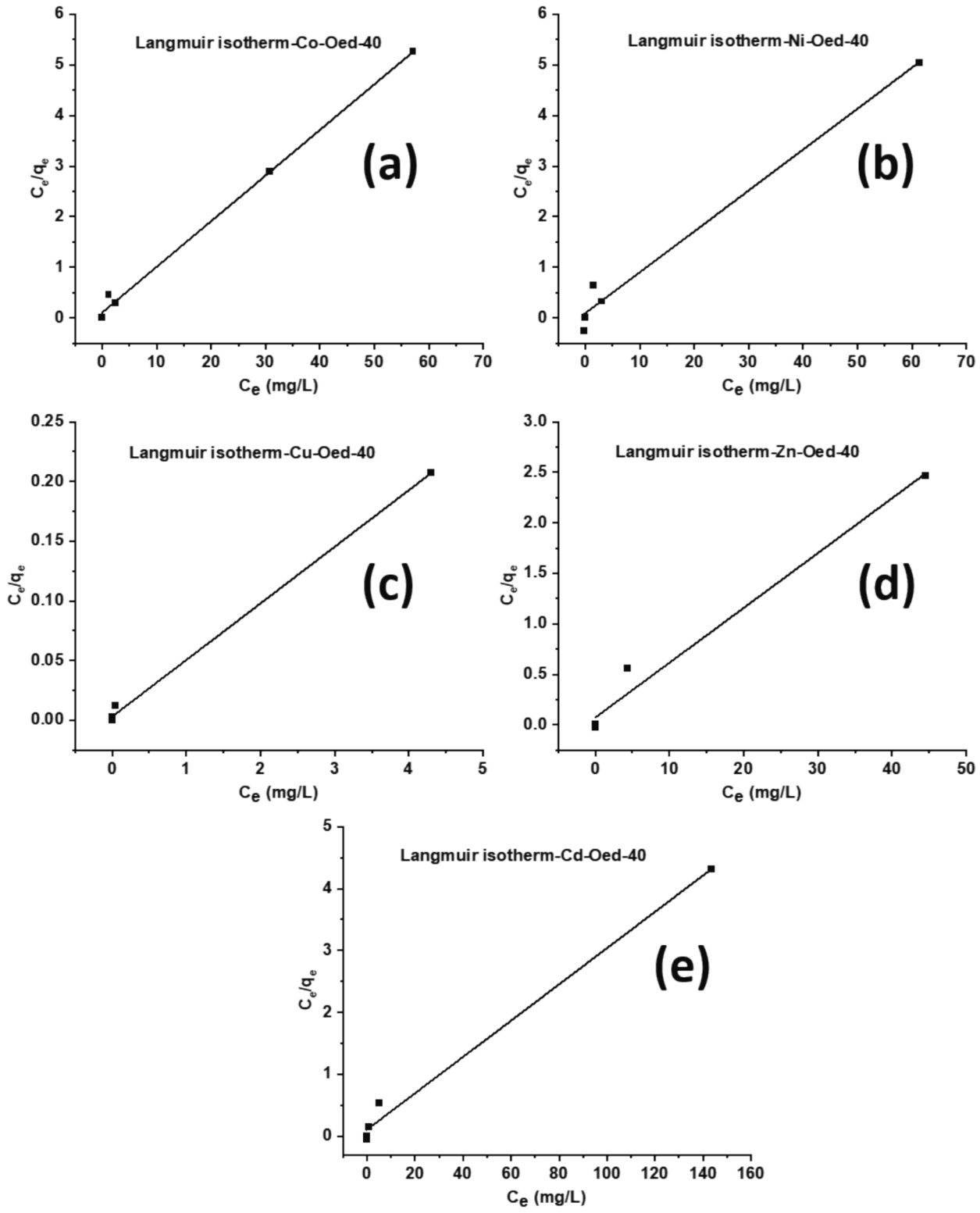

Fig. 10. Langmuir isotherm for Oed-40 biochar.

and Cd ions at different concentrations using 0.5 g of Oed-40 biochar are presented in Fig. 10 and Fig S4, respectively. The values of Langmuir and Freundlich constants and other parameters for all heavy metals are presented in Table 3. The results demonstrated that the correlation coefficient (R^2 = 0.981–0.998) fitted well with the Langmuir isotherm model compared to Freundlich model (R^2 = 0.816–0.918), indicating that monolayer adsorption means the maximum number of homogeneous active sites are present on the surface of Oed-40 biochar (Chaudhary et al., 2023). According to the Langmuir model, the maximum adsorption capacities calculated to be 9.33, 10.74, 322.58, 13.70 and 9.11 mg g^{-1} for Co, Ni, Cu, Zn and Cd, respectively. The Freundlich constant (KF)/adsorption capacity was calculated by using Freundlich model and the obtained values were 4.14, 2.94, 11.71, 5.15 and 6.68 mg g^{-1}, respectively. These results indicate that the Langmuir

Table 3
Fitting parameters of Langmuir and Freundlich isotherm models for adsorption of multiple heavy metals by Oed-40.

Biochar	Heavy metals	Langmuir Model			Freundlich Model		
		q_m (mg g^{-1})	K_L (L mg^{-1})	R^2	K_F (mg g^{-1})	n	R^2
Oed-40	Co	9.33	1.18	0.996	4.14	4.19	0.892
	Ni	10.74	1.15	0.984	2.94	2.84	0.816
	Cu	322.58	0.06	0.998	11.71	3.45	0.875
	Zn	13.70	1.34	0.981	5.15	2.85	0.873
	Cd	9.11	3.74	0.992	6.68	3.56	0.918

Table 4
Comparison of heavy metal adsorption capacities of different biochars.

Type of biochar	Heavy metals	Adsorption capacity (mg/g)	References
Enteromorpha biochar	Cu	2.54	(Yang et al., 2019)
Ascophyllum nodosum biochar	Cu	223	(Katiyar et al., 2021)
Macroalgal bloom biochar	Co, Ni, Cu, Cd	5.80, 5.74, 10.90, 16.28	(Jaiswal et al., 2021b)
Chlorella sorokiniana biochar	Co, Ni, Cu, Cd	9.43, 11.90, 14.08, 11.11	(Jaiswal et al., 2021a)
Mushroom-stick biochar	Cu, Cd, Ni	18.8, 11.2, 9.8	(Wang et al., 2019a)
Citrus Peel biochar	Cu, Cd	4.61, 15.46	(Chaudhary et al., 2023)
Brinjal stem biochar	Cu, Cd	246.31, 8.23	(Chaudhary et al., 2023)
Eichhornia crassipes bio-char	Zn, Cu, Cd	45.40, 48.20, 44.04	(Li et al., 2018)
Chitosan-coated gasifier biochar	Cu, Cd	111.5, 85.8	(Burk et al., 2020)
Sewage sludge bio-char	Zn, Cu	2.475, 5.415	(Zhou et al., 2017)
***Oedogonium* derived biochar**	**Co, Ni, Cu, Zn, Cd**	**9.33, 10.74, 322.58, 13.70, 9.11**	**This study**

model is more suitable than Freundlich model to describe the adsorption process of heavy metals.

3.2.5. Adsorption mechanism

Adsorption mechanism of heavy metals by *Oedogonium*-derived biochar is correlated with several interaction between the biochar and heavy metals in aqueous solutions. It is a mass transfer process for transferring the heavy metals from the solution to the biochar through physical and/or chemical exchanges. Based on the results of biochar characterization and adsorption isotherm, biochar's heavy metal adsorption mechanism mainly included cation exchange, surface complexation, electrostatic interactions, physical adsorption and precipitation (Li et al., 2017). The possible heavy metals adsorption mechanisms are discussed as follow: 1) Cation exchange: The heavy metal ions could be exchanged with the cations, for example Na^+, Ca^{+2}, K^+, Mg^{+2} available in Oed-40 biochar. 2) Surface complexation: Surface complexation involves the formation of coordination bonds between the surface functional groups (donor) and heavy metal ions (acceptor). The existence of oxygen-containing functional groups (e.g. C = O, O-H) on Oed-40 biochar surface could form complexes with heavy metal ions. 3) Electrostatic interactions: Positively charged heavy metals could interact with the negative charges on the surface-active sites of biochar via electrostatic forces. 4) Physical adsorption: Physical adsorption is a function of biochar's porous and disordered surface structures. The micro-mesoporous and disordered structure of Oed-40 biochar was one of the main critical factors to facilitate heavy metals fixation into the pores and channels through physicochemical adsorption. 5) Precipitation: The removal of heavy metals via precipitation mechanism is due to the influence of alkali, such as lime or NaOH, to adjust the pH of multiple heavy metal solutions to the lowest solubility of the revealed metals. In aqueous solution, metal hydroxide complexes may form due to the influence of pH, which leads to the precipitation of heavy metal complexes onto the surface of Oed-40.

To confirm the adsorption of heavy metals on Oed-40 biochar, the material was further characterized by SEM and FTIR after adsorption. As shown in Fig. S4, the SEM images of biochar is completely different from the biochar before adsorption (Fig. 1(e) and (f)). There are plenty of pores and channels were observed on the surface of biochar before adsorption of heavy metals. However, the porous and disordered structure disappeared after adsorption, indicating metal adsorption occurred on the surface of biochar. Fig. S5 shows the FTIR spectra to compare the properties of biochar with and without heavy metals adsorption by Oed-40. Several changes of peak positions were observed in the biochar before and after adsorption. In particular, the –OH peak shifted from 3290 to 3308 cm^{-1}, demonstrating that the biochar was involved in the adsorption process. In the meantime, when heavy metals adsorbed on the surface of Oed-40 biochar the peaks at 1007, 1408 and 1592 cm^{-1} not only shifted to 1014, 1414 and 1601 cm^{-1} but also lost the sharpness of peaks, further confirming the successful adsorption of heavy metals. A similar phenomenon also observed in the published literature (Liu et al., 2021).

The excellent adsorption capacity of heavy metals on Oed-40 is due to the relatively high specific surface area with the existence of micro-mesopores, presence of abundant surface functional groups, minerals and inhomogeneous structure, which SEM, BET, XRD, FTIR and Raman proved. Removing multiple heavy metals could be recognized as an integrated approach to surface phenomena and accessible functional groups. A comparative study on heavy metals adsorption using biochar obtained from different biomasses is shown in Table 4. Compared to most published results, *Oedogonium*-derived biochar demonstrated a higher adsorption capacity of five heavy metals.

In comparison with five heavy metals, the outstanding adsorption capacity of Cu (322.58 mg/g) is due to its higher affinity, which fascinated Cu to combine with oxygen-containing functional groups of biochar to form stable complexes even with several metal competitors present in the solution (Chen et al., 2015). The outcomes of heavy metal adsorption tests in the current study will promote the possibility of a practical application of *Oedogonium*-based biochar for wastewater treatment.

4. Conclusions

The current study aimed to investigate the removal of multiple heavy metals by *Oedogonium*-derived biochar. The physical and chemical properties of biochar are affected by pyrolysis time, which different characterization techniques have examined. Pyrolysis time, metal ion concentrations, and contact time considerably influence the adsorption of multiple heavy metals. Because of the distinguished properties, Oed-40 had exceptional adsorption capacity for five heavy metals. The Langmuir isotherm model and PSO kinetics were the best fit to elucidate the adsorption mechanism concerning monolayer adsorption that happened on the surface of Oed-40. The results indicate that the optimization of pyrolysis time was vital during the preparation of biochar from *Oedogonium* species. This strategy can be extended to prepare biochar from other algal biomasses to achieve the maximum adsorption capacity.

CRediT authorship contribution statement

Anjon Kumar Mondal: Writing – review & editing, Writing – original draft, Visualization, Methodology, Investigation, Formal analysis, Data curation, Conceptualization. **Cora Hinkley:** Writing – review & editing, Methodology, Formal analysis, Data curation. **Stalin Kondaveeti:** Writing – review & editing, Validation, Methodology, Investigation, Formal analysis, Data curation. **Phong H. N. Vo:** Writing – review

& editing, Data curation. **Peter Ralph:** Writing – review & editing, Validation, Supervision, Resources, Project administration. **Unnikrishnan Kuzhiumparambil:** Writing – review & editing, Visualization, Validation, Supervision, Resources, Project administration, Conceptualization.

Declaration of competing interest

The authors declare that they have no known competing financial interests or personal relationships that could have appeared to influence the work reported in this paper.

Data availability

Data will be made available on request.

Acknowledgements

Not applicable

Appendix A. Supplementary data

Supplementary data to this article can be found online at https://doi.org/10.1016/j.biortech.2024.131562.

References

Ahmad, M., Lee, S.S., Oh, S.-E., Mohan, D., Moon, D.H., Lee, Y.H., Ok, Y.S., 2013. Modeling adsorption kinetics of trichloroethylene onto biochars derived from soybean stover and peanut shell wastes. Environmental Science and Pollution Research 20, 8364–8373.

Alhashimi, H.A., Aktas, C.B., 2017. Life cycle environmental and economic performance of biochar compared with activated carbon: a meta-analysis. Resources, Conservation and Recycling 118, 13–26.

Arán, D.S., Deza, M., Monferrán, M.V., Pignata, M.L., Harguinteguy, C.A., 2023. Use of local waste for biochar production: Influence of feedstock and pyrolysis temperature on chromium removal from aqueous solutions. Integrated Environmental Assessment and Management 19 (3), 717–725.

Bilal, M., Ihsanullah, I., Younas, M., Shah, M.U.H., 2021. Recent advances in applications of low-cost adsorbents for the removal of heavy metals from water: a critical review. Separation and Purification Technology 278, 119510.

Biswal, B.K., Balasubramanian, R., 2023. Use of biochar as a low-cost adsorbent for removal of heavy metals from water and wastewater: a review. Journal of Environmental Chemical Engineering 110986.

Burk, G.A., Herath, A., Crisler, G.B., Bridges, D., Patel, S., Pittman Jr, C.U., Mlsna, T., 2020. Cadmium and copper removal from aqueous solutions using chitosan-coated gasifier biochar. Frontiers in Environmental Science 8, 541203.

Carolin, C.F., Kumar, P.S., Saravanan, A., Joshiba, G.J., Naushad, M., 2017. Efficient techniques for the removal of toxic heavy metals from aquatic environment: a review. Journal of Environmental Chemical Engineering 5 (3), 2782–2799.

Chakraborty, R., Asthana, A., Singh, A.K., Jain, B., Susan, A.B.H., 2022. Adsorption of heavy metal ions by various low-cost adsorbents: a review. International Journal of Environmental Analytical Chemistry 102 (2), 342–379.

Chaudhary, H., Dinakaran, J., Notup, T., Vikram, K., Rao, K.S., 2023. Comparison of adsorption performance of biochar derived from urban biowaste materials for removal of heavy metals. Environmental Management 1–17.

Chen, F., Hu, Y., Dou, X., Chen, D., Dai, X., 2015. Chemical forms of heavy metals in pyrolytic char of heavy metal-implanted sewage sludge and their impacts on leaching behaviors. Journal of Analytical and Applied Pyrolysis 116, 152–160.

Cho, S.-K., Igliński, B., Kumar, G., 2023. Biomass based biochar production approaches and its applications in wastewater treatment, machine learning and microbial sensors. Bioresource Technology, 129904.

Chowdhury, S., Mazumder, M.A.J., Al-Attas, O., Husain, T., 2016. Heavy metals in drinking water: occurrences, implications, and future needs in developing countries. Science of the Total Environment 569, 476–488.

Fazal, T., Faisal, A., Mushtaq, A., Hafeez, A., Javed, F., Alaud Din, A., Rashid, N., Aslam, M., Rehman, M.S.U., Rehman, F., 2021. Macroalgae and coal-based biochar as a sustainable bioresource reuse for treatment of textile wastewater. Biomass Conversion and Biorefinery 11, 1491–1506.

Hoslett, J., Ghazal, H., Ahmad, D., Jouhara, H., 2019. Removal of copper ions from aqueous solution using low temperature biochar derived from the pyrolysis of municipal solid waste. Science of the Total Environment 673, 777–789.

Jaiswal, K.K., Kumar, V., Verma, R., Verma, M., Kumar, A., Vlaskin, M.S., Nanda, M., Kim, H., 2021a. Graphitic bio-char and bio-oil synthesis via hydrothermal carbonization-co-liquefaction of microalgae biomass (oiled/de-oiled) and multiple heavy metals remediations. Journal of Hazardous Materials 409, 124987.

Jaiswal, K.K., Kumar, V., Vlaskin, M.S., Nanda, M., Verma, M., Ahmad, W., Kim, H., 2021b. Hydropyrolysis of freshwater macroalgal bloom for bio-oil and biochar production: kinetics and isotherm for removal of multiple heavy metals. Environmental Technology & Innovation 22, 101440.

Katiyar, R., Patel, A.K., Nguyen, T.-B., Singhania, R.R., Chen, C.-W., Dong, C.-D., 2021. Adsorption of copper (II) in aqueous solution using biochars derived from Ascophyllum nodosum seaweed. Bioresource Technology 328, 124829.

Kehrein, P., Van Loosdrecht, M., Osseweijer, P., Garfí, M., Dewulf, J., Posada, J., 2020. A critical review of resource recovery from municipal wastewater treatment plants–market supply potentials, technologies and bottlenecks. Environmental Science: Water Research & Technology 6 (4), 877–910.

Koçer, A.T., Özçimen, D., 2021. Determination of combustion characteristics and kinetic parameters of Ulva lactuca and its biochar. Biomass Conversion and Biorefinery 1–10.

Kumar, V., Parihar, R.D., Sharma, A., Bakshi, P., Sidhu, G.P.S., Bali, A.S., Karaouzas, I., Bhardwaj, R., Thukral, A.K., Gyasi-Agyei, Y., 2019. Global evaluation of heavy metal content in surface water bodies: A meta-analysis using heavy metal pollution indices and multivariate statistical analyses. Chemosphere 236, 124364.

Li, H., Dong, X., da Silva, E.B., de Oliveira, L.M., Chen, Y., Ma, L.Q., 2017. Mechanisms of metal sorption by biochars: Biochar characteristics and modifications. Chemosphere 178, 466–478.

Li, Q., Tang, L., Hu, J., Jiang, M., Shi, X., Zhang, T., Li, Y., Pan, X., 2018. Removal of toxic metals from aqueous solution by biochars derived from long-root Eichhornia crassipes. Royal Society Open Science 5 (10), 180966.

Liao, Q., Pan, W., Zou, D., Shen, R., Sheng, G., Li, X., Zhu, Y., Dong, L., Asiri, A.M., Alamry, K.A., 2018. Using of g-C3N4 nanosheets for the highly efficient scavenging of heavy metals at environmental relevant concentrations. Journal of Molecular Liquids 261, 32–40.

Liu, P., Rao, D., Zou, L., Teng, Y., Yu, H., 2021. Capacity and potential mechanisms of Cd (II) adsorption from aqueous solution by blue algae-derived biochars. Science of the Total Environment 767, 145447.

Lyu, H., Gong, Y., Gurav, R., Tang, J. 2016. Potential application of biochar for bioremediation of contaminated systems. in: *Biochar Application*, Elsevier, pp. 221-246.

McDonald-Wharry, J., Manley-Harris, M., Pickering, K., 2013. Carbonisation of biomass-derived chars and the thermal reduction of a graphene oxide sample studied using Raman spectroscopy. Carbon 59, 383–405.

Mondal, A.K., Hinkley, C., Krishnan, L., Ravi, N., Akter, F., Ralph, P., Kuzhiumparambil, U., 2024. Macroalgae-based biochar: preparation and characterization of physicochemical properties for potential applications. RSC Sustainability.

Oliveira, F.R., Patel, A.K., Jaisi, D.P., Adhikari, S., Lu, H., Khanal, S.K., 2017. Environmental application of biochar: Current status and perspectives. Bioresource Technology 246, 110–122.

Park, C.M., Han, J., Chu, K.H., Al-Hamadani, Y.A.J., Her, N., Heo, J., Yoon, Y., 2017. Influence of solution pH, ionic strength, and humic acid on cadmium adsorption onto activated biochar: experiment and modeling. Journal of Industrial and Engineering Chemistry 48, 186–193.

Poo, K.-M., Son, E.-B., Chang, J.-S., Ren, X., Choi, Y.-J., Chae, K.-J., 2018. Biochars derived from wasted marine macro-algae (Saccharina japonica and Sargassum fusiforme) and their potential for heavy metal removal in aqueous solution. Journal of Environmental Management 206, 364–372.

Qiu, B., Tao, X., Wang, H., Li, W., Ding, X., Chu, H., 2021. Biochar as a low-cost adsorbent for aqueous heavy metal removal: A review. Journal of Analytical and Applied Pyrolysis 155, 105081.

Roslee, A.N., Munajat, N.F., 2018. Comparative study on pyrolysis behavior and kinetics of two macroalgae biomass (Ulva cf. flexuosa and hy. edulis) using thermogravimetric analysis. J. Teknol 80 (2), 123–130.

Sanka, P.M., Rwiza, M.J., Mtei, K.M., 2020. Removal of selected heavy metal ions from industrial wastewater using rice and corn husk biochar. Water, Air, & Soil Pollution 231, 1–13.

Shaikh, W.A., Chakraborty, S., Islam, R.U., Ghfar, A.A., Naushad, M., Bundschuh, J., Maity, J.P., Mondal, N.K., 2022. Fabrication of biochar-based hybrid Ag nanocomposite from algal biomass waste for toxic dye-laden wastewater treatment. Chemosphere 289, 133243.

Singh, A., Sharma, R., Pant, D., Malaviya, P., 2021. Engineered algal biochar for contaminant remediation and electrochemical applications. Science of the Total Environment 774, 145676.

Staszak, K., Regel-Rosocka, M., 2024. Removing heavy metals: cutting-edge strategies and advancements in biosorption technology. Materials 17 (5), 1155.

Tan, X., Zhang, F., Wang, H., Ho, S.-H., 2023. The magic of algae-based biochar: advantages, preparation, and applications. Bioengineered 14 (1), 2252157.

Teh, Y.Y., Lee, K.T., Chen, W.-H., Lin, S.-C., Sheen, H.-K., Tan, I.S., 2017. Dilute sulfuric acid hydrolysis of red macroalgae Eucheuma denticulatum with microwave-assisted heating for biochar production and sugar recovery. Bioresource Technology 246, 20–27.

Truong, Q.-M., Nguyen, T.-B., Chen, W.-H., Chen, C.-W., Patel, A.K., Bui, X.-T., Singhania, R.R., Dong, C.-D., 2023. Removal of heavy metals from aqueous solutions by high performance capacitive deionization process using biochar derived from Sargassum hemiphyllum. Bioresource Technology 370, 128524.

Verma, M., Kumar, A., Singh, K.P., Kumar, R., Kumar, V., Srivastava, C.M., Rawat, V., Rao, G., Kumari, S., Sharma, P., 2020. Graphene oxide-manganese ferrite (GO-MnFe2O4) nanocomposite: One-pot hydrothermal synthesis and its use for adsorptive removal of Pb2+ ions from aqueous medium. Journal of Molecular Liquids 315, 113769.

Wang, X., Li, X., Liu, G., He, Y., Chen, C., Liu, X., Li, G., Gu, Y., Zhao, Y., 2019a. Mixed heavy metal removal from wastewater by using discarded mushroom-stick biochar:

adsorption properties and mechanisms. Environmental Science: Processes & Impacts 21 (3), 584–592.
Wang, Z., Liu, K., Xie, L., Zhu, H., Ji, S., Shu, X., 2019b. Effects of residence time on characteristics of biochars prepared via co-pyrolysis of sewage sludge and cotton stalks. Journal of Analytical and Applied Pyrolysis 142, 104659.
Wang, Y., Ma, C., Kong, D., Lian, L., Liu, Y., 2023. Review on application of algae-based biochars in environmental remediation: progress, challenge and perspectives. Journal of Environmental Chemical Engineering, 111263.
World Health, O. 2022. *Guidelines for drinking-water quality: incorporating the first and second addenda*. World Health Organization.
Xiang, W., Zhang, X., Chen, J., Zou, W., He, F., Hu, X., Tsang, D.C.W., Ok, Y.S., Gao, B., 2020. Biochar technology in wastewater treatment: A critical review. Chemosphere 252, 126539.
Xiao, Y., Xue, Y., Gao, F., Mosa, A., 2017. Sorption of heavy metal ions onto crayfish shell biochar: effect of pyrolysis temperature, pH and ionic strength. Journal of the Taiwan Institute of Chemical Engineers 80, 114–121.
Yang, W., Wang, Z., Song, S., Han, J., Chen, H., Wang, X., Sun, R., Cheng, J., 2019. Adsorption of copper (II) and lead (II) from seawater using hydrothermal biochar derived from Enteromorpha. Marine Pollution Bulletin 149, 110586.
Yu, K.L., Lau, B.F., Show, P.L., Ong, H.C., Ling, T.C., Chen, W.-H., Ng, E.P., Chang, J.-S., 2017. Recent developments on algal biochar production and characterization. Bioresource Technology 246, 2–11.
Zhao, J.J., Shen, X.J., Domene, X., Alca Niz, J.M., Liao, X., Palet, C., 2019. Comparison of biochars derived from different types of feedstock and their potential for heavy metal removal in multiple-metal solutions. Sci. Rep 9, 1–12.
Zhou, D., Liu, D., Gao, F., Li, M., Luo, X., 2017. Effects of biochar-derived sewage sludge on heavy metal adsorption and immobilization in soils. International Journal of Environmental Research and Public Health 14 (7), 681.